

**Annual Report, 2000**  
**SOUTHERN CALIFORNIA EARTHQUAKE CENTER**

**Title of Project:** RELM: Earthquake Potential Models

**Name of PI:** Steven N. Ward

**Institution:** University of California, Santa Cruz

Much of my SCEC funded research in 2000 dealt with initial development of several maps of earthquake potential/earthquake probability in support of SCEC's Regional Earthquake Likelihood Models (RELM) program. RELM has asked its participants to generate a range of "well documented and physically defensible" models of earthquake rate density based on inputs from geology, seismicity, geodesy, and computer simulation. One goal of the program is to assess the impact, or lack of impact, that certain assumptions inherent to earthquake potential assessment (fault segmentation or  $M_{\max}$  for instance) have on earthquake hazard. I offer three classes of earthquake potential maps — one based purely on geodesy, one based purely on geology, and one based on computer simulations of earthquakes on the fault system of southern California.

### Geodetic Models

#### Motivation.

Until recently, earthquake rate estimation was entirely the realm of geologists and seismologists. With well-defined faults and sufficiently frequent earthquakes, geology, historical seismicity and paleoseismology can furnish fairly reliable earthquake statistics. More commonly, questionable fault numbers, fault geometries, fault slip rates and scattered seismicity characterize the situation, and earthquake statistics do not reveal themselves readily. For most of the world, historical seismicity and paleoseismology can not constrain earthquake statistics to the degree necessary for an acceptable rate assessment. Today, information from space geodesy patches some of these voids. Space geodetic monitoring quantifies potential earthquake activity within the network even if that activity occurs on faults that are unknown, too slowly slipping, or too deep to study by conventional geological or seismological techniques. Geodesy's most valuable contributions in estimating earthquake rates spring from:

- its ability to provide rates of earthquakes on faults that are undocumented or unobservable by traditional methods;
- its ability to provide independent verification of the rates of deformation in regions where geologists have documented faults; and
- its ability to provide a means to judge the consistency of the contemporary deformation field and the historical earthquake record.

Technical description. The RELM geodetic models employ GPS site velocities from SCEC Velmap2, SOPAC and the USGS. Horizontal site velocities are first mapped into maximum geodetic strain rates

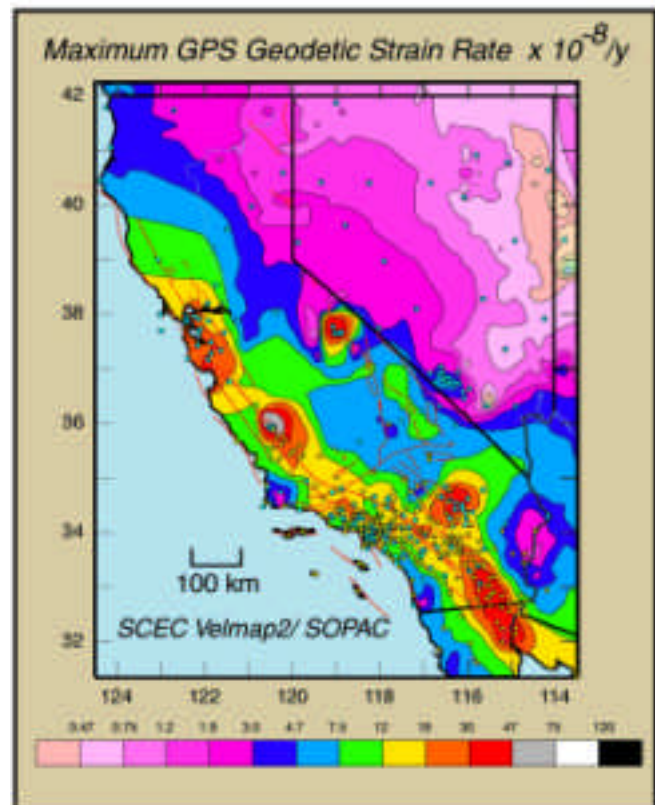
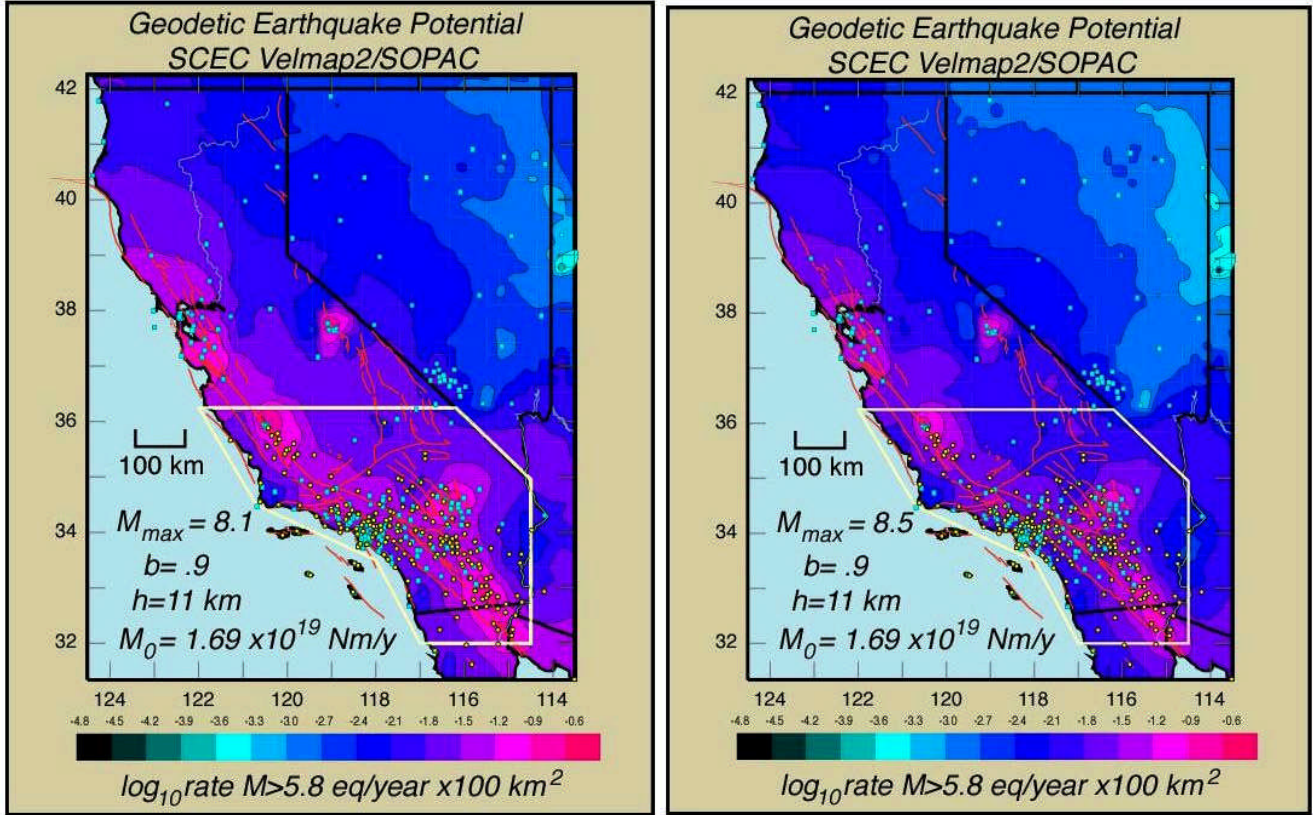


**Figure 1.** Contour map of maximum GPS geodetic strain rate shown in units of  $\times 10^{-8}/y$ .

$$\dot{\epsilon}_{\max}(\mathbf{r}) = \max[\text{abs}(\dot{\lambda}_1(\mathbf{r})), \text{abs}(\dot{\lambda}_2(\mathbf{r}))] \quad (1)$$



**Figures 2 and 3.**  $\log_{10}$  rate of earthquakes  $M > 5.8$  per year per  $100 \text{ km}^2$  obtained from **Figure 1**. Geodetic moment rate at each point is assumed to be released in earthquakes that follow a Gutenberg - Richter relation ( $b=0.9$ ) truncated at  $M_{\max}=8.1$  (left) and  $M_{\max}=8.5$  (right).

taking care to remove rotations (see Figure 1). The  $\dot{\epsilon}_1$  and  $\dot{\epsilon}_2$  here are the eigenvalues of the horizontal strain rate tensor. The maximum geodetic strain rate is then translated into geodetic moment rate density using Kostrov's formula per unit area

$$\dot{M}_{\text{geodetic}} = 2\mu H_s \dot{\epsilon}_{\text{max}} \quad (2)$$

Geodetic moment rate density connects to geodetic strain rate through seismogenic thickness,  $H_s$ . The  $H_s$  equal to 11 km used in these calculations gives a total geodetic moment rate budget for southern California of  $1.7 \times 10^{19} \text{ Nm/y}$ . Finally, moment rate density becomes earthquake rate density under the assumption that (2) distributes into earthquakes that follow a truncated Gutenberg-Richter distribution of given  $b$ -value and  $M_{\max}$ . The mean recurrence interval for magnitude  $M+$  events is thus

$$T_{>}(M) = \frac{b}{1+b} \frac{10^{(1.5+b)M_{\max}+9.05}}{\dot{M}_{\text{geodetic}} [10^{bM_{\max}} - 10^{bM}]} \quad (3)$$

Figures 2 and 3 show typical earthquake potential maps in the form of  $\log_{10}$  rate of earthquakes  $M > 5.8$  per year per  $100 \text{ km}^2$  obtained for  $b=0.9$  and  $M_{\max}=8.1$  and  $M_{\max}=8.5$ . Figure 4 plots the total rate of predicted seismicity from these geodetic models and compares them with observed seismicity. Either model makes for a reasonable fit.

**Required Information:** (1) GPS site positions, horizontal velocities and errors. (2) Map of seismogenic thickness.  $H_s$  can be scaled to meet regional moment rate constraints. (3) A b-value and  $M_{max}$ .

**Advantages:** (1) Being purely strain rate based, geodetic models are very 'clean' with few subjective constraints. (2) The maps have well defined error bounds and (3) Wide geographical coverage even in areas where little fault information is known.

**Drawbacks:** (1) Mapping of geodetic strain to seismic strain is not unique. Some strain may be aseismic slip or non-tectonic. (2) Patterns of instantaneous strain may not reflect the long-term situation over a full earthquake cycle.

**Geological Models**

**Motivation.** At least one member in the RELM spectrum has to be purely geological because worldwide, estimating earthquake potential from direct interpretation of active faults is still the most wide-spread approach. Also, because most of the information in the geological models is shared with the earthquake simulation models, geologically-based earthquake potential maps form a base for comparison.

**Technical description.** Fault-based earthquake potential assessments differ from geodetic-based ones in that only those locations that have a specified fault have earthquake potential. For RELM, I include all southern California faults that slip at rates greater than or equal to 1 mm/y – some 3,600 km in all. Fault traces are smoothed versions of the CDMG database (See Figure 5). A moment rate per unit length of fault is first computed from the fault's slip rate, downdip width and a rigidity value. Next, moment rate per unit fault length is turned into moment rate density by area-averaging with a Gaussian filter with a span of several tens of km. Lastly, maps of moment rate density are turned into earthquake potential maps by distributing the moment rate density into earthquakes of various magnitudes. Ultimately, for well known faults, this distribution could be based on actual rupture mode statistics. Currently however, I just use (3) again (See Figure 6).

**Geodetic Earthquake Potential Southern California Total**

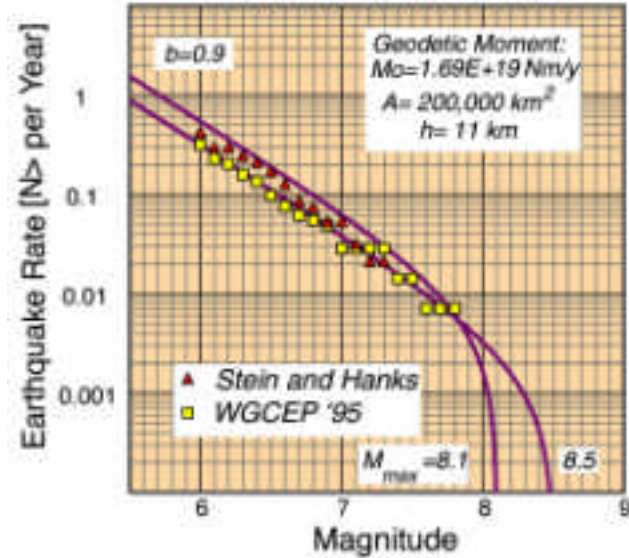


**Figure 4.** Total seismicity rates for southern California predicted by the earthquake potential models of Figures 2 and 3. The stars and squares are the observed rates as estimated by WGCEP'95 and Stein and Hanks.

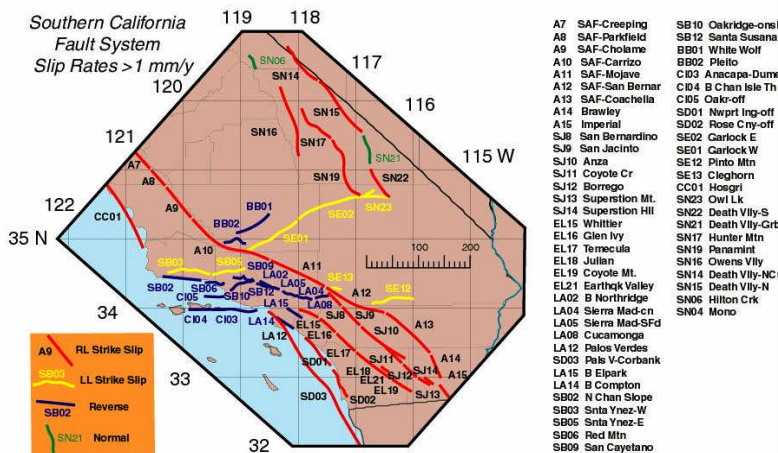


**Figure 5.** Map of the southern California fault system including all faults with slip rates greater than or equal to 1 mm/y. These faults form the primary input for both the geologic and computer simulation based earthquake potential models.

earthquake potential maps by distributing the moment rate density into earthquakes of various magnitudes. Ultimately, for well known faults, this distribution could be based on actual rupture mode statistics. Currently however, I just use (3) again (See Figure 6).

**Required Information:** (1) Maps of fault traces with a resolution of a km or two. (2) Orientation of the faults (if not vertical). (3) Down dip seismogenic depth. (4) Style of slip. (5) Slip Rates. (6) Rupture mode statistics if known, otherwise a  $M_{max}$  and b-value for use in G-B relation.

**Advantages:** Earthquake potential falls near known faults.

**Drawbacks:** (1) Geologists will never be able to specify every fault location, much less their slip rates and rupture mode behaviors. (2) No time dependence.

### Physical Earthquake Simulation Model

**Motivation.** A fundamental problem that makes the prediction of earthquake behaviors more difficult than other types of predictions in the physical sciences is lack of samples. Large earthquakes occur just too infrequently on any given fault to glean a reliable understanding of earthquake characteristics. Because of this fundamental under sampling, scientists must turn to alternative approaches to advance the field. One alternative that holds promise is earthquake simulations; that is, physically-based computer models of earthquake recurrence.

Earthquake potential models based on computer simulations follow those that I have produced for the faults of the San Francisco Bay Area (Ward, 2000). For RELM, I include all southern California faults that slip at rates greater than or equal to 1 mm/y (Figure 5 again). Faults with dips less than 90 degrees are replaced by vertical surfaces – a concession to the 2-D nature of my simulations. Even with these concessions, the simulation operates with, and inverts, 1000 x 1000 matrices -- about the limit of what can be done on a low-end workstation.

**Technical description.** All seismicity simulations involve a balance between fault driving stress and fault frictional resistance. When the scale is tipped in favor of fault driving stress, an earthquake must occur to reestablish balance. On faults, physical laws govern both stress accumulation and stress rebalancing by earthquakes. Keeping track of, and occasionally rebalancing, fault stresses in obedience with physical laws is the essence of earthquake simulation. Earthquake simulation requires five elements: (1) a regional earth structure, (2) a set of faults to embed in this structure, (3) a means to apply tectonic loading stresses to these faults between earthquakes, (4) a means to transfer stresses from fault to fault during earthquakes, and (5) a means to decide when and where an earthquake should start, and how big it should grow to when it does start (i.e. fault friction law). To some extent, all of these elements are available currently, and I have created a prototype earthquake model (Figure 7). To make the model tractable within current capacity computers, the prototype admits several simplifications. Among these are 2-D geometry and a quasi-static assumption. Nevertheless, the prototype serves as tangible evidence that realistic earthquake simulations can be constructed even now.

For applications to RELM, earthquakes listed in long synthetic catalogs will be turned into earthquake potential maps like Figure 6 by a smoothing operation. Note that because the simulation model and the geological model employ the same sets of faults and slip rates, they have identical moment rate density distributions. The primary difference in the models is how the moment rate is partitioned into earthquakes. The simulation automatically supplies this information based on physical fault parameters. In the geological models, the partitioning has to be prescribed.

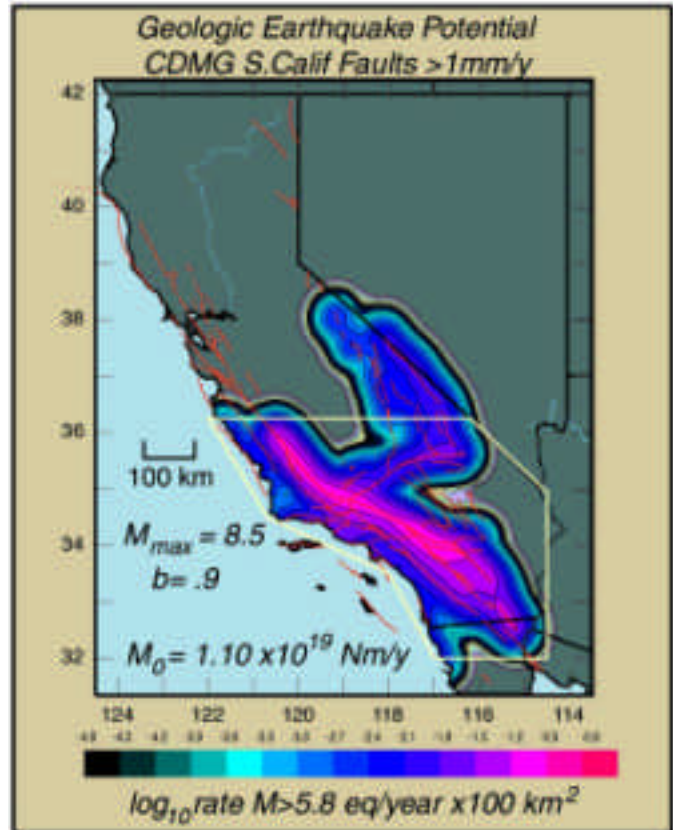


**Figure 6.**  $\log_{10}$  rate of earthquakes  $M > 5.8$  per year per 100  $\text{km}^2$  obtained from the faults of **Figure 5** under the assumption that the geologic moment rate at each fault point is released in earthquakes that follow a Gutenberg-Richter relation ( $b=0.9$ ) truncated at  $M_{\max}=8.5$ . The total moment rate budget for southern California in this model is of  $1.1 \times 10^{19}$   $\text{Nm/y}$ .

## Earthquake Simulation on the Southern California Fault System - Years 457-728

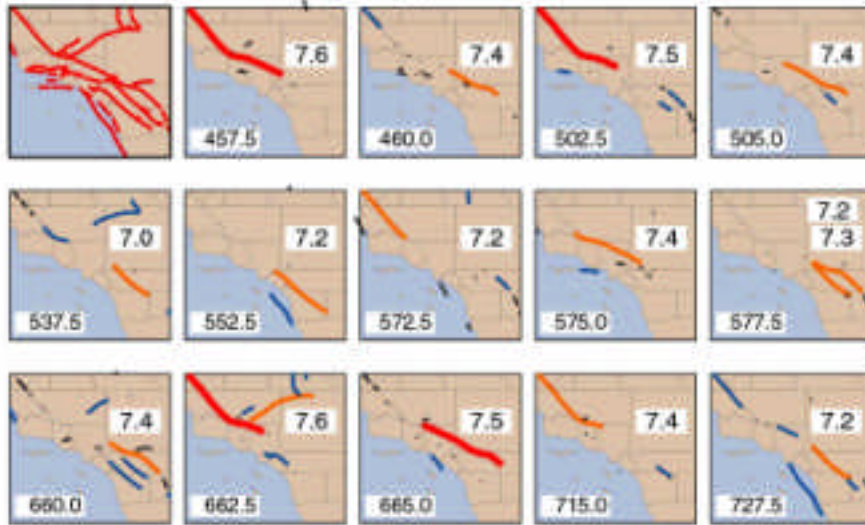


**Figure 7.** Initial attempt at a computer model of southern California earthquakes. The included faults appear in red in the upper left panel. The “movie” frames are not regularly spaced in time, but update on the occurrence of an  $M > 7$  event listed to the upper right in each frame. Red coloring marks  $M > 7.5$  earthquakes; orange coloring,  $7 < M < 7.5$ ; and the thick and thin black lines,  $6.5 < M < 7$  and  $6 < M < 6.5$  respectively. At the lower left in each panel is time in years since the start of the simulation.

Comparisons between predicted and observed bulk seismicity (Figure 8) provide a check on model effectiveness. The overproduction of earthquakes near  $M 6.5$  relative to the observed rate, indicates that fault strengths and friction parameters in this prototype need adjustment.

**Advantages:** (1) Earthquake potential falls near known faults. (2) Partition of moment rate into earthquake rate determined from physical laws. (3) Potential to supply time-dependent statistics.

**Drawbacks:** (1) Geologists will never be able to specify every fault location and slip rates, (2) Very time consuming to compute.

### SCEC Publications in 2000-2001:

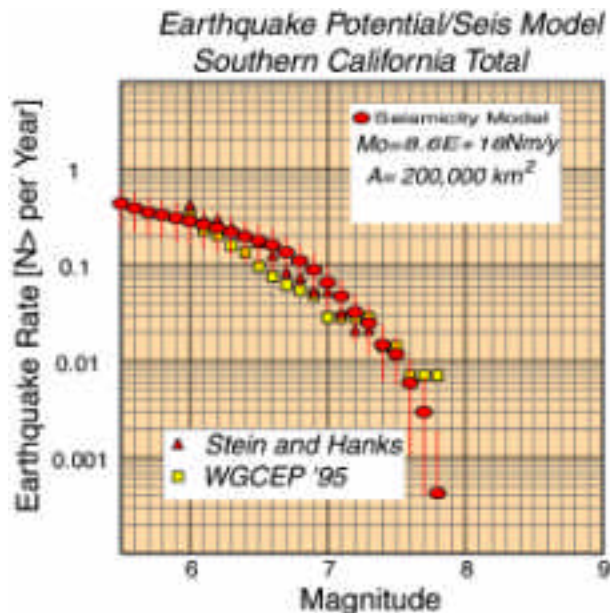


**Figure 8.** Annual rate of earthquakes greater than magnitude  $M$  as produced by the computer simulation.

Ward, S. N., 2000. San Francisco Bay Area Earthquake Simulations: A step toward a Standard Physical Earthquake Model, *Bull. Seism. Soc. Am.*, 90, 370-386.

Ward, S. N. and E. Asphaug, 2000. Asteroid Impact Tsunami: A probabilistic hazard assessment, *Icarus*, 145, 64-78.

Ward, S. N., 2001. “Tsunamis” in *The Encyclopedia of Physical Science and Technology*, ed. R. A. Meyers, Academic Press, Accepted and In Press.

Ward, S. N., 2001. Landslide Tsunami, *J. Geophys. Res.*, Accepted and In Press.

Ward, S. N. and E. Asphaug, 2001. Impact Tsunami - Eltanin, *Deep-Sea Research*, Accepted and In Press.

Ward, S. N., 2001. Asteroid Cratering Coverage: A Probabilistic Approach, *J. Geophys. Res.*, Submitted August 2000.

Ward, S. N. and S. Day 2001. Cumbre Vieja Volcano -- Potential Collapse and Tsunami at La Palma, Canary Islands, *Geophys. Res. Lett.*, In preparation for March 2001.